Brigham Young University
BYU ScholarsArchive

Faculty Publications

2006-01-01

Microwave observations of daily Antarctic sea-ice edge expansion and contraction rates

David G. Long
david_long@byu.edu

Jeffrey R. Allen

Follow this and additional works at: https://scholarsarchive.byu.edu/facpub

 Part of the Electrical and Computer Engineering Commons

Original Publication Citation

Allen, J. R., and D. G. Long. "Microwave Observations of Daily Antarctic Sea-Ice Edge Expansion and Contraction Rates." Geoscience and Remote Sensing Letters, IEEE 3.1 (26): 54-8

BYU ScholarsArchive Citation

Long, David G. and Allen, Jeffrey R., "Microwave observations of daily Antarctic sea-ice edge expansion and contraction rates" (2006). *Faculty Publications*. 329.
https://scholarsarchive.byu.edu/facpub/329

This Peer-Reviewed Article is brought to you for free and open access by BYU ScholarsArchive. It has been accepted for inclusion in Faculty Publications by an authorized administrator of BYU ScholarsArchive. For more information, please contact ellen_amatangelo@byu.edu.

Microwave Observations of Daily Antarctic Sea-Ice Edge Expansion and Contraction Rates

Jeffrey R. Allen and David G. Long, *Senior Member, IEEE*

***Abstract*—Algorithms for estimating sea-ice extent from remotely sensed microwave sensor data can benefit from knowledge of the "*a priori*" distribution of the daily expansion and contraction of the sea-ice pack. To estimate the probability distribution of daily Antarctic sea-ice extent change, two independent sea-ice datasets are analyzed: sea-ice extent derived from the QuikSCAT scatterometer and ice concentration estimates from the Special Sensor Microwave/Imager. The daily sea-ice advance and retreat is tracked over a four-year period. The distribution of the daily sea-ice advance/retreat from each sensor is similar and is approximately double-exponential. Daily ice-pack statistics are presented.**

***Index Terms*—SeaWinds, QuikSCAT, Special Sensor Microwave/Imager (SSMI), sea ice.**

I. Introduction

GIVEN the importance of the role Antarctic sea-ice plays in climate, monitoring its extent is critical. A number of current microwave sensors make daily global observations of sea-ice cover. In particular, the SeaWinds scatterometer on QuikSCAT collects radar backscatter observations, and the Special Sensor Microwave/Imager (SSM/I) radiometer collects brightness temperature (T_b) measurements. Based on these observations, sea-ice extent can be estimated directly from the observations using algorithms which employ detection techniques to classify areas as sea-ice or open ocean [1]–[3] or by thresholding the estimated ice concentration [4]. Direct detection algorithms are often termed "ice-masking" methods and are based on statistical inference techniques. The performance of such methods is affected by the statistical models and assumptions employed. For example, the accuracy of existing ice-masking methods can be improved with knowledge of the prior distribution of the daily expansion and contraction of the sea-ice. Lacking previously published daily distributions, we desire to use remote sensing data to estimate the statistics of sea-ice advance/retreat over a 24-h period.

Changes in the Antarctic sea-ice edge have been researched extensively through detection [5], [6], Markov models [7], [8], and relationships to global climatic events [9], [10]; however, such studies have been focused on long-term ice-extent and ice-edge forecasting. In contrast, we are interested in the probability distribution of the daily sea-ice extent change as a function of longitude in order to provide useful prior distributions for ice-masking methods. Such data have not been previously published to our knowledge.

Manuscript received March 2, 2005; revised July 11, 2005.

The authors are with the Microwave Earth Remote Sensing Laboratory, Brigham Young University, Provo, UT 84602 USA (e-mail: long@ee.byu.edu).

Digital Object Identifier 10.1109/LGRS.2005.856710

To provide this information, in this letter we estimate the probability distribution of daily Antarctic sea-ice expansion and contraction from two sensors, one active (the SeaWinds scatterometer) and the other passive (the F13 SSM/I radiometer). From the daily sea-ice extent reported by each sensor we employ a finite difference approach over a relatively large dataset (1999–2003) to estimate the latitudinal daily sea-ice change and other statistics. This letter is organized as follows. A brief description of the data sources and sea-ice extent processing is provided in Section II. Section III summarizes the results, and a conclusion is provided in Section IV.

II. Data

A. QuikSCAT Sea-Ice Detection

We begin our study of daily Antarctic sea-ice advance and retreat by utilizing sea-ice information reported by the SeaWinds scatterometer on QuikSCAT (hereafter referred to as simply QuikSCAT). QuikSCAT, whose mission began Julian Day (JD) 200, 1999 and continues today (2005), is an active sensor that transmits Ku-band signals on two polarizations [vertical (v) and horizontal (h)] and measures the return echo power, or backscatter, from the Earth's surface. QuikSCAT reports daily coverage for the entire Antarctic region. From these observations the sea-ice edge is located by first creating an image of the average daily radar cross section (RCS) using the scatterometer reconstruction (SIR) algorithm [11]. Then, in this letter, the Remund–Long (R–L) ice-masking algorithm [2] is used to to classify pixels as either open ocean or sea-ice and create a binary sea-ice extent mask. Finally, image edge detection techniques [12] are employed to locate the latitudinal extent of the ice-edge in the binary image along each longitudinal line displayed in Fig. 1 The pixel resolution of the images and ice masks is 4.45 km/pixel.

B. SSM/I Sea-Ice Detection

We also use sea-ice data provided by the SSM/I radiometer F-13. SSM/I is a passive instrument that observes T_b over several channels and polarizations. The sensor provides daily coverage of the entire Antarctic region at 25-km resolution [13].

In order to estimate sea-ice extent we employ images provided by the National Snow and Ice Data Center (NSIDC), in which the National Aeronautics and Space Administration (NASA) Team algorithm has been employed to detect the sea-ice concentration percentage [4]. The images provide daily coverage of the entire Antarctic region at 25 km/pixel. We classify pixels with sea-ice concentration greater or equal to a threshold as ice, and pixels with less than the threshold as

1545-598X/$20.00 © 2006 IEEE

Authorized licensed use limited to: Brigham Young University. Downloaded on February 3, 2009 at 10:36 from IEEE Xplore. Restrictions apply.

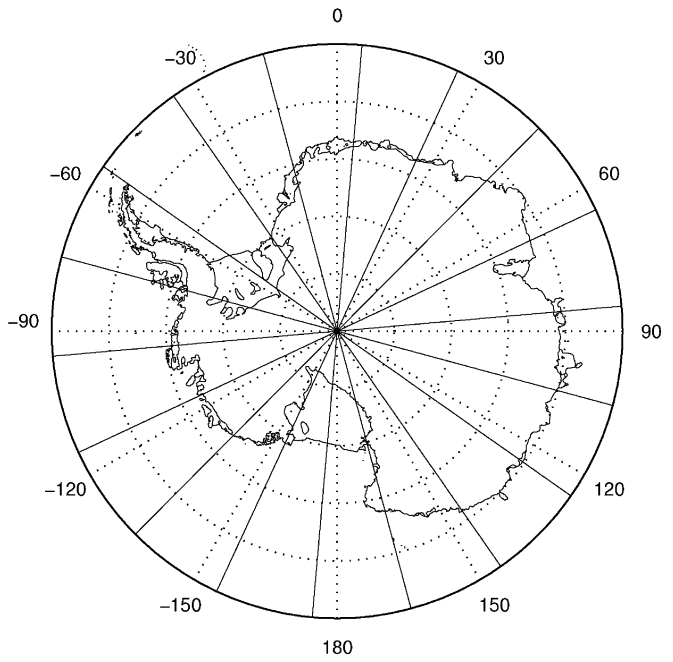

Fig. 1. Polar map of Antarctica. The longitude study lines are the solid lines pointing radially outward from center.

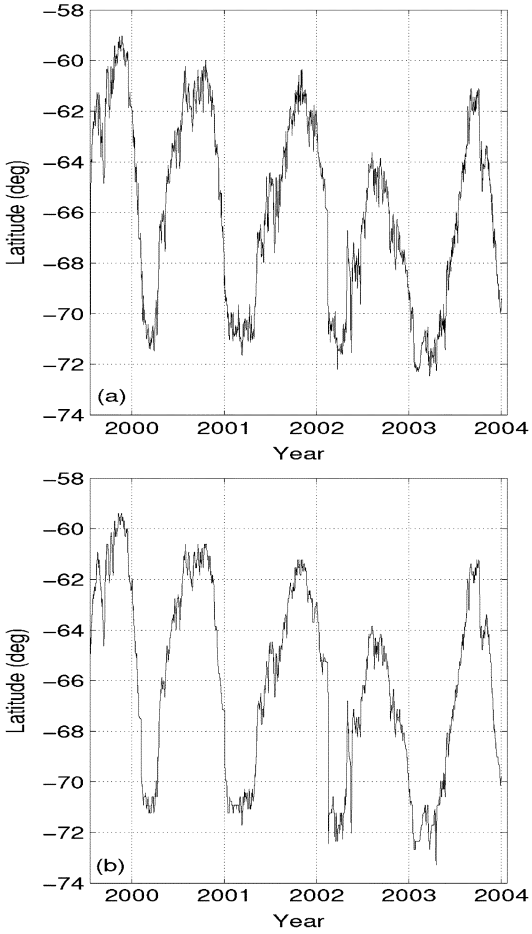

Fig. 2. Time series of daily (a) QuikSCAT and (b) SSM/I observations of the Antarctic latitudinal ice extent along 135°W longitude.

open ocean. Previous studies have shown that, in general, an ice concentration threshold of 30% best matches QuikSCAT and SSM/I ice-edges [2], though some seasonal variation has been noted due to the differences in the sensitivity of active and passive sensors to sea ice [1]. For this letter a 30% threshold is used.

As with QuikSCAT, the daily advance and retreat of the ice-edge estimated by SSM/I is determined by performing edge detection and plotting the edge position as a function of time. In this way, we may compare the ice-edges detected by both sensors and estimate distributions and statistics.

III. Results

For each of the instruments and meridional study lines, we track the daily change in the sea-ice edge as a function of latitude. To remove errors and spurious misclassifications, a robust 3-σ filter [14] is applied to the data. As a representative of normal ice-edge movement, Fig. 2 displays the QuikSCAT and SSM/I sea-ice edge latitudinal extent along 135°W longitude. While, in general, the ice-edge determined by both sensors is well correlated, discrepancies exist between the sensors' observations. These are due to resolution differences (discussed later) and the differences between passive and active sea-ice detection, which are discussed in many publications, e.g., [15]–[17]. SSM/I measures brightness temperature, which is a function of physical temperature and emissivity. Emissivity is strongly dependent on the liquid fraction of ice concentration [17]. On the other hand, microwave scattering of wet surfaces at off-nadir incidence angles is dominated by the surface roughness. Thus, some ice structures, readily observed by SSM/I, may not be observed by QuikSCAT and vice versa [3], [6].

To estimate the probability distribution function (pdf) of the daily sea-ice advance/retreat, histograms of the daily sea-ice edge change are created. Fig. 3 displays the sea-ice edge change histogram along 135°W longitude with a graph of the pdf of a double exponential function with the same mean and variance as the sea-ice data. We observe that for both sensors the distribution of the sea-ice edge change is approximately double-exponential. Similar results are obtained for other longitudes.

The QuikSCAT and SSM/I histograms in Fig. 3 are very similar but exhibit some differences. The ice edge changes detected by SSM/I have fewer extreme values and the histogram created from QuikSCAT has somewhat greater spread. In addition to the active/passive sensor sensitivities previously discussed, sensor resolution differences may play a role: the higher resolution in the masks provided by QuikSCAT allows greater precision in sea-ice advance/retreat detection. To illustrate the effects of pixel size on sea-ice advance/retreat, Fig. 4 displays a plot of the daily latitudinal change of the SSM/I and QuikSCAT observed ice-edge along 135°W. The SSM/I changes exhibit pixel quantization effects that are not easily observed in the corresponding QuikSCAT plot. We note that many of the SSM/I daily changes are exactly ± 35.4 km, the diagonal length of the 25×25 km SSM/I pixel, and are the result of diagonal ice edge movement of a single pixel.

To investigate the effects of pixel size on ice-edge retrieval, we analyze daily ice-edge advance/retreat based on QuikSCAT ice-masks reduced to lower resolution. The lower resolution

Authorized licensed use limited to: Brigham Young University. Downloaded on February 3, 2009 at 10:36 from IEEE Xplore. Restrictions apply.

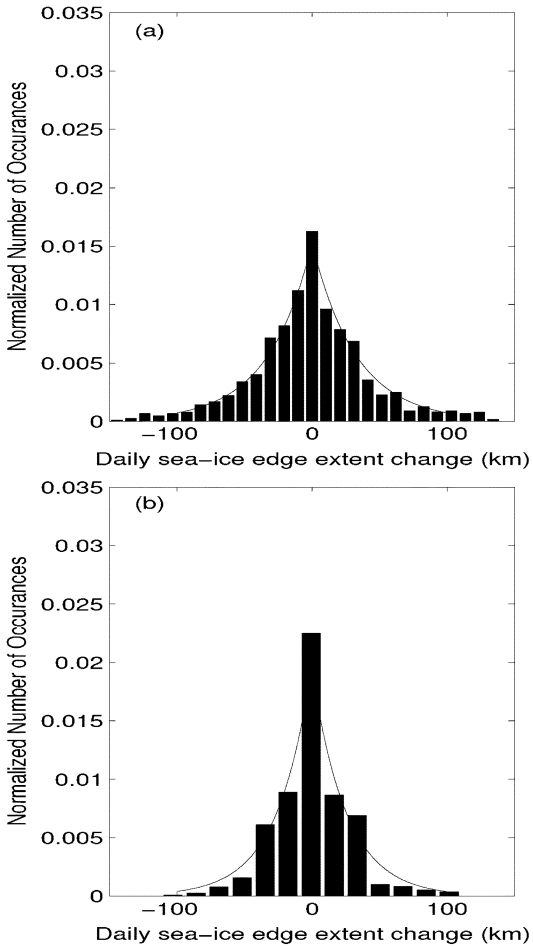

Fig. 3. Histograms of (a) QuikSCAT- and (b) SSM/I-observed daily sea-ice expansion along 135°W and double-exponential pdfs with the same mean and variance as the histograms. The standard deviations are 40.9 km for QuikSCAT and 28.0 km for SSM/I. The differences in the bin resolution of the histograms reflect the differences in the spatial resolution of the sensors.

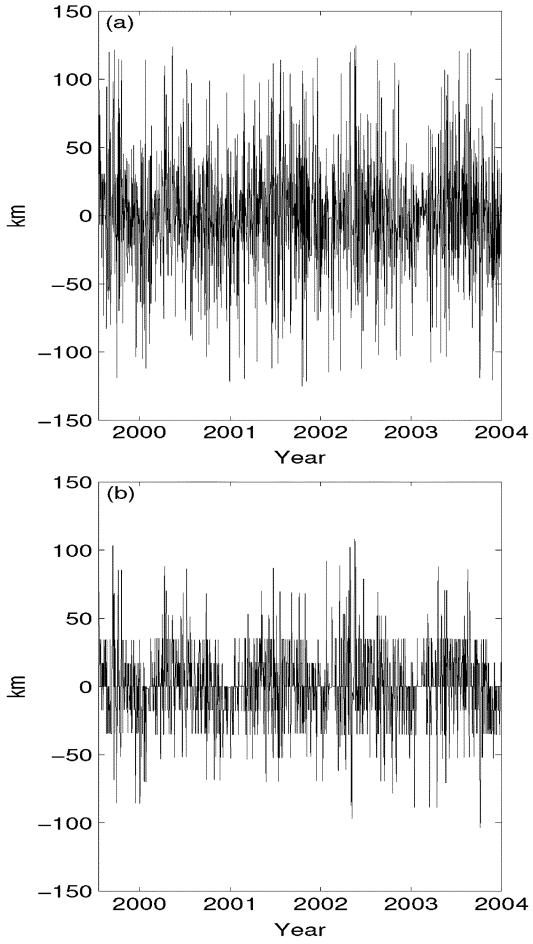

Fig. 4. Time series of daily change of the (a) QuikSCAT- and (b) SSM/I-observed ice edge along 135°W longitude.

masks are created by grouping 5×5 pixel blocks into single pixels. Ocean/ice classification of the new pixels is determined by the state of the majority of the 25 original pixels. This approach produces 22.5×22.5 km pixels that are comparable with the 25×25 km SSM/I pixels. Fig. 5 displays the daily changes and daily change histograms of the reduced resolution QuikSCAT ice masks along 135°W longitude. While the quantized QuikSCAT and the SSM/I histograms in Figs. 5 and 3 are similar, the tails of the quantized QuikSCAT histogram are larger, suggesting that irrespective of the resolution, the QuikSCAT ice edge is more variable than the SSM/I edge.

The latitudinal ice extent and daily change histograms allow us to estimate several ice expansion statistics for each study longitude. These statistics are summarized in Tables I and II and include the following parameters:

- *Daily Change Std.:* standard deviation of the daily (day-to-day) sea-ice advance/retreat.
- *Mean Absolute Daily Change:* average absolute daily advance/retreat of the ice.
- *Mean Contraction Season Daily Change:* average sea-ice change during the contraction season, defined as the period between JD 300 of a given year to JD 50 of the following year as inferred from [18].
- *Mean Dilation Season Daily Change:* average sea-ice change during the dilation season, defined to be between JD 100-200 of a given year as inferred from [18].
- *Average Annual Change:* average difference between the maximum and minimum sea-ice edge extent for each year.

Additionally, Table II, displays the percent difference between the QuikSCAT and SSM/I statistics, and the correlation coefficient of the sea-ice extents observed by the sensors.

We note that the QuikSCAT observed daily change std. and mean absolute daily change are generally 30% to 40% larger than the corresponding SSM/I statistics. As previously discussed, we attribute these discrepancies primarily to the sensitivity differences between passive and active sea-ice detection discussed further in [1], [15]–[17]. Sensor noise may also play a role. These results suggest that further investigation of the relative performance of active and passive systems in mapping sea-ice extent is warranted.

Fig. 6 displays each sensor's mean absolute daily change and daily change std. as a function of longitude above a plot of the Antarctic coastline. This is compared to the annual variation. The largest daily changes occur in the Weddell Sea and near the West Ice Shelf where the largest annual change also occurs.

Authorized licensed use limited to: Brigham Young University. Downloaded on February 3, 2009 at 10:36 from IEEE Xplore. Restrictions apply.

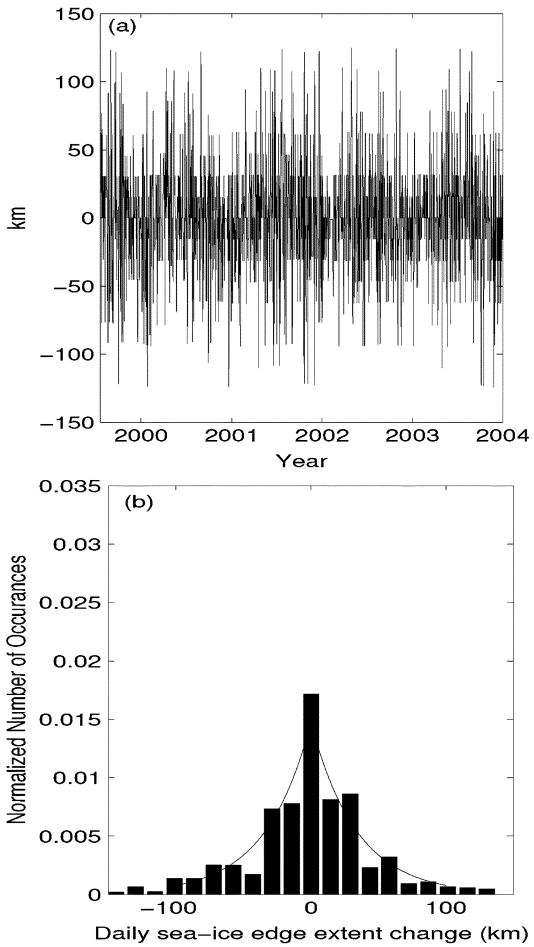

Fig. 5. (a) Daily change of the reduced resolution QuikSCAT ice masks. (b) Histogram of the daily changes in the observed ice edge along 135°W longitude and a double-exponential pdf with the same mean and variance as the histogram. The standard deviation is 41 km.

TABLE I
MEASURED QUIKSCAT SEA-ICE EXTENT VALUES FOR EACH OF THE STUDY LONGITUDES. VALUES ARE IN KILOMETERS

Longitudinal Line	Daily Change Std.	Mean Absolute Daily Change	Mean Contraction Season Daily Change	Mean Dilation Season Daily Change	Average Annual Change
-175°	38.6	28.2	-2.93	4.17	1436
-155°	40.7	29.7	-7.69	8.11	1271
-135°	40.9	30.1	-6.45	6.35	1234
-115°	39.4	28.4	-2.18	3.50	914
-95°	34.8	25.5	-3.60	2.84	726
-75°	34.2	24.4	-3.40	4.36	782
-55°	6.8	1.8	-0.00	0.54	138
-35°	42.6	31.0	-7.64	4.96	1476
-15°	40.8	30.0	-7.22	7.54	1698
5°	41.7	30.2	-4.03	10.2	1813
25°	40.5	29.4	-5.35	6.52	1719
45°	35.7	25.2	-5.75	5.33	1086
65°	36.3	25.5	-2.76	4.56	1006
85°	43.9	31.5	-3.07	4.26	971
105°	34.2	23.7	-1.91	3.26	716
125°	27.4	18.8	-1.21	1.05	540
145°	31.1	21.2	0.74	1.71	587
165°	30.6	20.5	-2.33	4.40	708

TABLE II
MEASURED SSM/I SEA-ICE EXTENT STATISTICAL VALUES FOR EACH OF THE STUDY LONGITUDES. THE PERCENT DIFFERENCE BETWEEN THE CORRESPONDING QUIKSCAT AND SSM/I VALUES FOR EACH STATISTIC ARE SHOWN IN PARENTHESIS. VALUES, EXCEPT THE UNITLESS CORRELATION COEFFICIENT AND THE PERCENTAGES, ARE IN KILOMETERS

Longitudinal Line	Daily Change Std.	Mean Absolute Daily Change	Mean Contraction Season Daily Change	Mean Dilation Season Daily Change	Average Annual Change	Corr. Coefficient
-175°	27.3 (-29)	18.2 (-36)	-4.30 (47)	5.04 (21)	1473 (3)	0.964
-155°	27.6 (-32)	19.5 (-34)	-6.21 (-19)	8.29 (2)	1285 (1)	0.984
-135°	28.0 (-31)	19.0 (-37)	-5.65 (-12)	7.51 (18)	1188 (-4)	0.992
-115°	25.4 (-36	17.3 (-39)	-2.81 (29)	3.79 (8)	914 (0)	0.957
-95°	23.7 (-32)	15.8 (-38)	-2.77 (-23)	3.21 (13)	684 (-6)	0.973
-75°	23.6 (-31)	15.7 (-36)	-3.38 (-1)	4.85 (11)	751 (-4)	0.980
-55°	5.2 (-24)	0.9 (-51)	0.00 (-100)	0.65 (21)	120 (-13)	0.845
-35°	23.2 (-45)	15.2 (-51)	-3.64 (-52)	8.07 (63)	1337 (-9)	0.975
-15°	23.6 (-42)	15.9 (-47)	-4.49 (-38)	9.95 (32)	1665 (-2)	0.981
5°	28.2 (-32)	17.9 (-41)	-6.30 (56)	10.90 (7)	1764 (-3)	0.989
25°	26.6 (-34)	17.2 (-42)	-5.25 (-2)	8.61 (32)	1686 (-2)	0.990
45°	21.3 (-40)	13.8 (-45)	-4.95 (-14)	5.33 (0)	1063 (-2)	0.985
65°	20.3 (-44)	13.5 (-47)	-3.00 (9)	4.86 (7)	961 (-5)	0.983
85°	24.6 (-44)	16.3 (-48)	-2.52 (-18)	6.39 (50)	915 (-6)	0.973
105°	20.0 (-42)	13.1 (-45)	-2.99 (56)	3.43 (5)	622 (-13)	0.959
125°	18.3 (-33)	12.0 (-36)	-1.78 (47)	2.02 (92)	458 (-15)	0.896
145°	19.5 (-37)	12.8 (-40)	-0.41 (-156)	2.44 (42)	573 (-2)	0.940
165°	18.9 (-38)	12.0 (-41)	-2.18 (-7)	5.24 (19)	701 (-1)	0.978

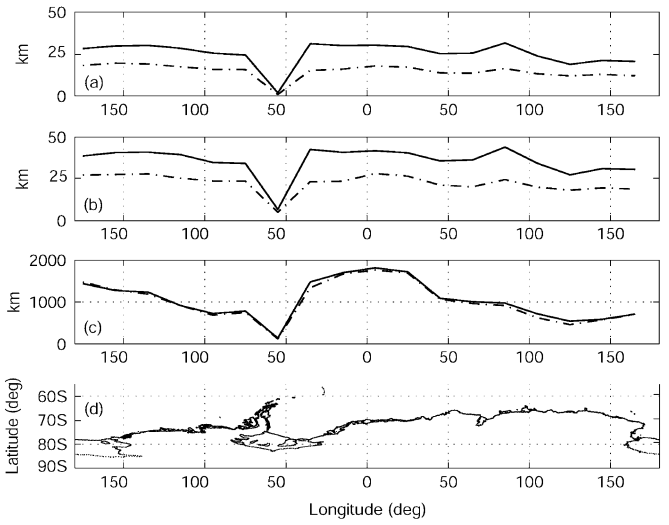

Fig. 6. Plots of (a) the mean absolute daily change, (b) daily change std., and (c) average seasonal change for (solid line) QuikSCAT and (dashed line) SSM/I sea-ice observations, and (d) the Antarctic coastline.

Similarly, the smallest daily changes occur near the Antarctic Peninsula where the annual change is the smallest. The large changes in the Weddell sea are expected as considerable variability and periods of rapid change are often observed in this area [18]. We also note that the ice along 85°E is prone to much larger changes than its neighbors. This effect is due to a large coastal polynya near Prydz Bay that serves as an area of high ice production. Thus, this area has a greater autumn sea-ice extent

Authorized licensed use limited to: Brigham Young University. Downloaded on February 3, 2009 at 10:36 from IEEE Xplore. Restrictions apply.

and a smaller midwinter extent than its neighbors [18]. Sea-ice near the Antarctic Peninsula generally consists of coastal fast ice with low seasonal variation [18], which is reflected by small changes in the ice-edge.

IV. Conclusion

The QuikSCAT scatterometer and the SSM/I radiometer are utilized to estimate the distribution of daily sea-ice edge advance and retreat in the Antarctic. The goal of this study is to generate daily statistics information for improving existing sea-ice detection algorithms by providing simple "*a priori*" probability distributions for daily ice extent change.

Analyzing several derived ice-edge advance/retreat statistics, we observe that the distribution of the sea-ice edge advance/retreat is approximately double exponential. Additionally, we find that the daily ice edge advance during the dilation season is generally larger than the retreat during the contraction season, a result consistent with previous research [18]. Ice growth and decay in the Antarctic are driven by a combination of ocean heat flux and shortwave radiation absorbed in leads opened by divergent ice conditions [5].

We note that the standard deviation of the daily sea-ice edge change as detected by the active QuikSCAT sensor is larger by 30% to 45% than determined by the passive SSM/I sensor for which a fixed (30%) ice concentration threshold is used to detect the ice extent. The sensor variation is attributed primarily to the differences in the sensitivity of the microwave ocean/ice signatures.

Acknowledgment

QuikSCAT SIR image data and ice-masks were obtained from the NASA Scatterometer Climate Record Pathfinder [19] project (http://www.scp.byu.edu). They were generated from data obtained from the Physical Oceanography Distributed Data Archive (PO.DAAC) at the Jet Propulsion Laboratory, Pasadena, CA. SSM/I ice concentration images were obtained from the National Snow and Ice Data Center (NSIDC). This work was completed at the Brigham Young University Microwave Earth Remote Sensing Laboratory.

References

[1] H. Anderson and D. Long, "Sea ice mapping method for seawinds," *IEEE Trans. Geosci. Remote Sens.*, vol. 43, no. 3, pp. 647–657, Mar. 2005.

[2] Q. Remund and D. Long, "Sea ice mapping algorithm for QuikSCAT and seawinds," in *Proc. IGARSS*, vol. 3, 1998, pp. 1686–1688.

[3] J. Haarpaintner, R. T. Tonboe, D. G. Long, and M. L. V. Woert, "Automatic detection and validity of the sea-ice edge: An application of enhanced-resolution QuikSCAT/Seawinds data," *IEEE Trans. Geosci. Remote Sens.*, vol. 42, no. 7, pp. 1433–1443, Jul. 2004.

[4] D. Cavalieri, P. Gloerson, and J. Zwally, "DMSP SSM/I daily polar gridded sea ice concentrations," Nat. Snow and Ice Data Center, Boulder, CO, J. Maslanik and J. Stroeve, Eds., 1990. Digital media: updated 2004 Jul. 1999 to Dec. 2003.

[5] M. Drinkwater and X. Liu, "Seasonal to interannual variability in Antarctic sea-ice surface melt," *IEEE Trans. Geosci. Remote Sens.*, vol. 38, no. 4, pp. 1827–1842, Jul. 2000.

[6] Y. Zhao, A. Liu, and D. Long, "Validation of sea ice motion from QuikSCAT with those from SSM/I and buoy," *IEEE Trans. Geosci. Remote Sens.*, vol. 40, no. 6, Jun. 2002.

[7] D. Chen and X. Yuan, "A Markov model for seasonal forecast of Antarctic sea ice," *J. Clim.*, vol. 17, pp. 3156–3168, 2004.

[8] J. Liu, X. J. Yuan, D. G. Martinson, and D. Rind, "Re-evaluating Antarctic sea-ice variability and its teleconnections in a GISS global climate model with improved sea ice and ocean processes," *Int. J. Climatol.*, vol. 24, pp. 841–852, 2004.

[9] X. Yuan and D. Martinson, "Antarctic sea ice variability and its global connectivity," *J. Clim.*, vol. 13, pp. 849–871, 2000.

[10] ——, "The Antarctic dipole and its predictability," *Geophys. Res. Lett.*, vol. 28, pp. 3609–3612, 2001.

[11] D. Early and D. Long, "Image reconstruction and enhanced resolution imaging from irregular samples," *IEEE Trans. Geosci. Remote Sens.*, vol. 39, no. 2, pp. 291–302, Feb. 2001.

[12] A. K. Jain, *Fundamentals of Digital Image Processing*. Upper Saddle River, NJ: Prentice-Hall, 1989.

[13] J. Hollinger, J. Pierce, and G. Poe, "SSM/I instrument evaluation," *IEEE Trans. Geosci. Remote Sens.*, vol. 28, no. 5, pp. 781–790, Sep. 1990.

[14] J. Lee, "Digital image smoothing and the sigma filter," *Comput. Vis., Graph., Image Process.*, vol. 24, no. 2, pp. 255–269, Nov. 1983.

[15] J. Grandell, J. Johannessen, and M. Halikainene, "Development of a synergetic sea ice retrieval method for the ERS-1 AMI wind scatterometer and SSM/I radiometer," *IEEE Trans. Geosci. Remote Sens.*, vol. 37, no. 2, pp. 668–679, Mar. 1999.

[16] S. Nghiem *et al.*, "Diurnal thermal cycling effects on microwave signatures of thin sea ice," *IEEE Trans. Geosci. Remote Sens.*, vol. 36, no. 1, pp. 111–124, Jan. 1998.

[17] D. Barber *et al.*, "Evolution of electromagnetic signatures of sea ice from inital formation to the establishment of thich first year sea ice," *IEEE Trans. Geosci. Remote Sens.*, vol. 36, no. 5, pp. 1642–1654, Sep. 1998.

[18] P. Gloersen *et al.*, *Arctic and Antarctic Sea Ice, 1978–1987: Satellite Passive-Microwave Obersvations and Analysis*. Greenbelt, MD: NASA Goddard Space Flight Center, 1992.

[19] D. Long, M. Drinkwater, B. Holt, S. Saatchi, and C. Bertoia, "Global ice and land climate studies using scatterometer image data," *Trans. Amer. Geophys. Union*, vol. 82, no. 43, p. 503, Oct. 2001.

Authorized licensed use limited to: Brigham Young University. Downloaded on February 3, 2009 at 10:36 from IEEE Xplore. Restrictions apply.